

## *Retraction*

# **Retracted: Dynamic Synchronization Modeling and Simulation of Video Sensing Nodes Based on Internet of Things**

### **Wireless Communications and Mobile Computing**

Received 18 July 2023; Accepted 18 July 2023; Published 19 July 2023

Copyright © 2023 Wireless Communications and Mobile Computing. This is an open access article distributed under the Creative Commons Attribution License, which permits unrestricted use, distribution, and reproduction in any medium, provided the original work is properly cited.

This article has been retracted by Hindawi following an investigation undertaken by the publisher [1]. This investigation has uncovered evidence of one or more of the following indicators of systematic manipulation of the publication process:

- (1) Discrepancies in scope
- (2) Discrepancies in the description of the research reported
- (3) Discrepancies between the availability of data and the research described
- (4) Inappropriate citations
- (5) Incoherent, meaningless and/or irrelevant content included in the article
- (6) Peer-review manipulation

The presence of these indicators undermines our confidence in the integrity of the article's content and we cannot, therefore, vouch for its reliability. Please note that this notice is intended solely to alert readers that the content of this article is unreliable. We have not investigated whether authors were aware of or involved in the systematic manipulation of the publication process.

Wiley and Hindawi regrets that the usual quality checks did not identify these issues before publication and have since put additional measures in place to safeguard research integrity.

We wish to credit our own Research Integrity and Research Publishing teams and anonymous and named external researchers and research integrity experts for contributing to this investigation.

The corresponding author, as the representative of all authors, has been given the opportunity to register their agreement or disagreement to this retraction. We have kept a record of any response received.

### **References**

- [1] Z. Wang and Y. Q. Wang, "Dynamic Synchronization Modeling and Simulation of Video Sensing Nodes Based on Internet of Things," *Wireless Communications and Mobile Computing*, vol. 2022, Article ID 2845786, 8 pages, 2022.

## Research Article

# Dynamic Synchronization Modeling and Simulation of Video Sensing Nodes Based on Internet of Things

Zeyu Wang  and Yu Qing Wang 

Department of Communication Design, Dankook University, 16890, Republic of Korea

Correspondence should be addressed to Yu Qing Wang; 201804328@stu.ncwu.edu.cn

Received 2 June 2022; Revised 21 June 2022; Accepted 1 July 2022; Published 21 July 2022

Academic Editor: Balakrishnan Nagaraj

Copyright © 2022 Zeyu Wang and Yu Qing Wang. This is an open access article distributed under the Creative Commons Attribution License, which permits unrestricted use, distribution, and reproduction in any medium, provided the original work is properly cited.

In order to solve the dynamic synchronization problem of IoT video perception, the authors propose an abstract model DSAM based on IoT video perception. This method firstly establishes the abstract model DSAM of IoT video perception based on the  $\pi$  network and then analyzes the state evolution, model transition, and dynamic interaction of the model; finally, the model DSAM is used to analyze and simulate the example. The result shows that when the model DSAM is tested and verified and when the number of buffer media is 50, 100, and 200, the minimum number of underflows of the DSAM model is 2 and the minimum video data packet loss rate is 1.02; the results are better than those of the MTFSC and 3TFSC models; in addition, without synchronization control, the synchronization rate between video frames is lower than that with synchronization control. The test results show that the model proposed and established by the authors can correctly handle the dynamic synchronization of IoT video perception and has certain practical value.

## 1. Introduction

A video image perception system is mainly to detect and recognize moving objects or targets and can be widely used in various fields of security protection, such as campus, transportation, and family. At present, there are certain researches and applications on video image perception systems at home and abroad. However, the algorithm and hardware design are complex, the implementation cost is high, the communication protocol adopts a private protocol, and the versatility is poor [1].

As one of the industries in the national development strategy, the Internet of things industry in China has developed rapidly with the support of central and local policies, and its scale has increased year by year. The Internet of things technology has played an important role in the fields of intelligent transportation, intelligent logistics, intelligent building, intelligent security, and intelligent home [2]. For example, smart home products combine technologies such as computer networks and automated control systems and realize the perception and remote control of various house-

hold devices. The smart grid uses intelligent means to realize the efficient use of energy and the security of energy supply through the digital information network system. Smart buildings construct a safe, efficient, and convenient building environment through the comprehensive application of various types of intelligent information [3]. It can be seen that IoT devices have penetrated into all aspects of our lives, and the impact of IoT devices is also growing. Some IoT devices carry a large amount of private data of the majority of users, and whether some IoT devices work normally or not, it is related to the personal and property safety of users and the safety production of enterprises [4]. Some past cases always remind us that IoT devices are generally vulnerable.

As an important part of the new generation of information technology, the Internet of things is a combination of various information equipment (such as RFID radio frequency identification devices, various sensors, and GPS or Beidou positioning systems), wireless transmission technology, and Internet technology, according to the agreed agreement, a network technology that realizes information exchange and communication of related items to realize

intelligent identification, positioning, tracking, monitoring, and management. As an application expansion of the Internet, the core of the development of the Internet of things is application innovation [5], as shown in Figure 1.

## 2. Literature Review

Although the Internet of things is still in the initial stage of development, most countries in the world have invested in a certain degree of technology, standards, application demonstrations, and business models and have achieved certain results [6]. As early as 2009, IBM launched the concept of “Smarter Planet”; the ideal effect of this solution is through the combination of a sensor network and Internet technology, changing the way of communication between people or between people and organizations to achieve thorough perception, extensive interconnection, and in-depth intelligence. Since then, top companies in various industries in the United States have also joined the IoT industry, aimed at improving the company’s operational efficiency; many enterprise applications such as automatic remote meter reading systems, item tracking, and security systems for power companies have emerged. In Europe, the European Commission has formally formulated the Internet of things as a strategic development plan for European ICT. As a result of the EU’s high emphasis on and strong support for the Internet of things, the application market of the Internet of things industry is relatively mature, especially in the Western European market; IoT applications have been realized in many fields such as safety monitoring, automotive information communication, public transportation, urban informatization, and industrial automation [7].

In the Internet of things, the most basic is the information and data perception of the underlying nodes; in the case of reliable hardware, there is still a failure of the intelligent sensing node. Among the reasons for the failure of the IntelliSense node, the most important issue is the software reliability of IntelliSense nodes. With the development of the times, the reliability growth model of software can be divided into classic type, imperfect debugging type (imperfect debugging), testing workload type (testing effort), change point type (change point), and other types of models. On the whole, research based on analytical methods accounts for a very large proportion [8]. Intelligent perception has been widely used and is an important infrastructure in the field of IoT perception. Intelligent sensing nodes integrate sensing information collection, real-time information processing, and real-time communication, such as the Internet of vehicles in the field of intelligent transportation; if a fault or accident occurs on the road, the intelligent perception system will perceive and process information such as location and environmental conditions in real time and transmit the processed information in real time for fast processing. Intelligent sensing nodes have high performance, such as brand-new, wide coverage and strong real-time characteristics, such as mutual communication and interoperability. Moreover, IntelliSense nodes have constraints in terms of power consumption, volume, and processor speed [9]. Qin et al. conducted an in-depth study on time-

extended Petri nets and described reliability by using their good scalability. Finally, a relatively perfect time-expanded Petri net SRG model evaluation scheme was formed, and it was applied to the actual embedded modeling process with good results [10]. Pan et al. studied the partition of software and hardware with dual-objective multichoice and proposed a heuristic algorithm to generate approximate solutions quickly, using a custom tabu search algorithm, an improved approximate solution algorithm, and a dynamic programming algorithm that quickly computes an exact solution; the hardware and software partitioning is studied [11]. Sabol et al. studied the partitioning of software and hardware under variable demands of intelligent systems and proposed a set of partitioning algorithms for enhanced hardware/software resource sharing parameters. Sabol et al. studied the hardware and software partitioning of heterogeneous multi-processor system-on-chip (MPSoC) and proposed an optimized integer linear programming algorithm to solve small input hardware and software A method for partitioning the problem [12].

The authors use the  $\pi$  network combined with the Petri net and the  $\pi$  calculus, establish the abstract model DSAM of the Internet of things video perception system, and realize the modeling of the dynamic synchronization of the IoT video perception system; being able to correctly handle the dynamic synchronization concurrency of IoT video perception has certain practical value [13].

## 3. Research Methods

*3.1. Model Establishment.* The IoT video perception system is a typical concurrent dynamic system. Using the  $\pi$  network, a dynamic synchronization abstract model DSAM (Dynamic Synchronization Abstract Model) for IoT video perception is established to describe its dynamic synchronization characteristics [14].

*Definition 1.* Define DSAM as a  $\pi$  network, that is,

$$\text{DSAM} = (C_p, X, T_t, C_f). \quad (1)$$

$C_p$  represents a basic token Petri net system, which is a collection of video perception libraries for the Internet of things;  $X = \{X_1, X_2, X_3, \dots\}$  represents a collection of interactive buttons, which is a collection of changes in the video perception information of the Internet of things, and different buttons represent different changes; and  $C_p \cap X = \phi$ ;  $T_t$  represents the time relationship set of the synchronous transition of IoT video perception, which is the arc set of the network DSAM, and  $T_t \subseteq (C_p \times X)(X \times C_p)$ ;  $C_f$  is an attribute function defined above, which represents the set of mapping relationships of the location set.

$C_p$  is a six-tuple; that is,  $C_p = (P, T, B, F, I_D, M : M_0)$  is a basic Petri net, and there are only two types of positions in the net: “normal” and “master.” Among them,  $P$  is a set of positions;  $T$  is a set of transitions;  $B : P \times T \rightarrow I, I = \{1, 2, 3, \dots\}$  is a set of directed arcs from positions to transitions;  $F : T \times P \rightarrow I, I = \{1, 2, 3, \dots\}$ , representing the set of

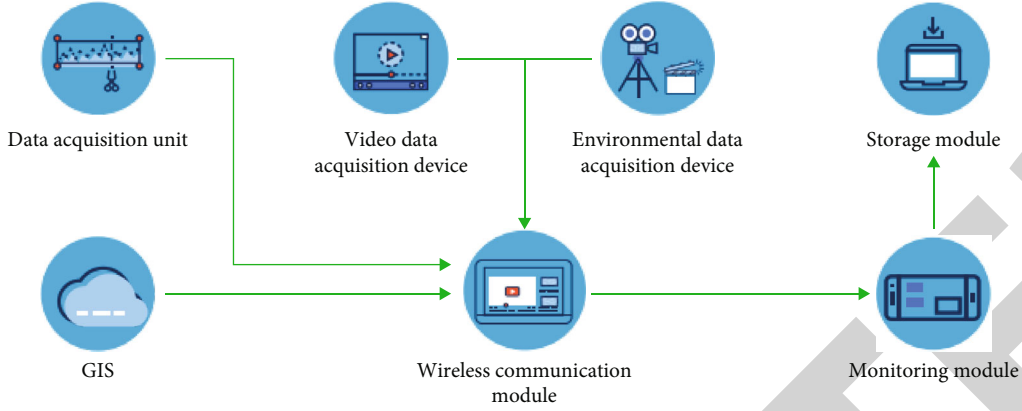


FIGURE 1: Video-aware node dynamics of the Internet of things.

directed arcs from transition to position;  $M : P \rightarrow I$  is the identification of the network system;  $I = \{0, 1, 2, \dots\}$ ;  $M_0$  are the initial identification;  $I_D$  is the OPN (Object-oriented Petri Net) element, namely,  $I_D = (C_{jp}, R_{token}, E_\pi)$ , where  $C_{jp}$  is the element defined by the basic Petri net and  $R_{token}$  is the token of  $C_{jp}$ ;  $E_\pi$  is the evolution factor of the DSAM model described by the calculus [15].

$X = \{X_1, X_2, X_3, \dots\}$  is an interactive button set; there are six kinds of buttons: “Skip,” “Pause,” “Back,” “Replay,” “Restart,” and “Modify Speed.”

$T_t$  mainly describes the set of time relations of the synchronous time transition of the IoT video perception system, and  $T_t$  can be formally defined by using TPN (Time Petri Net). DSAM conforms to the definition of the  $\pi$  network and is a  $\pi$  network. It needs to be defined here to better describe the DSAM model [16].

**Definition 2.**  $T_t$  is a time relationship set, which is an extension of a TPN network, that is,

$$T_t = (P_k, T_{dt}, Q_d, F_{kz}, F_{df}, S_{tbl}, W_{ma}, G_{bx}). \quad (2)$$

Among them,  $P_k$  is a collection of limited places of the Internet of things video perception system.  $T_{dt} = \{t_{dt1}, t_{dt2}, \dots, t_{dtn}\}$  is a limited set of temporal dynamic changes of the IoT video perception system and satisfies the condition  $P_k \cup T_{dt} \neq \emptyset, P_k \cap T_{dt} \neq \emptyset$ .  $Q_d = \{q_{d1}, q_{d2}, \dots, q_{dn}\}$  represents the limited transition set of various information data in the IoT video perception system and satisfies clause  $P_k \cap Q_d \neq \emptyset, Q_d \cap T_{dt} \neq \emptyset$ .  $F_{kz} \subseteq (P_k \times T_{dt}) \cup (T_{dt} \times P_k) \cup (P_k \times Q_d)$  is the set of arcs that control flow, and  $F_{df} \subseteq (P_k \times Q_d) \cup (Q_d \times P_k) \cup (P_k \times T_{dt})$  is a collection of arcs of the data flow, representing the dynamic relationship of the system.  $S_{tbl}$  is the mapping from  $T_{dt}$  to synchronization transition rules.  $W_{ma} : T_{dt} \rightarrow P_k$ , that is, the mapping relationship between the dynamic time transition set and the finite place, and it satisfies  $\forall p_k \in \{\text{master}\}, \exists t_{dti} \in T_{dt} | W_{MA}(t_{dti}) = p_k$ .  $F_{if} : T_{dt} \rightarrow (R + \cup \infty)$  which is the time mapping function, and  $R +$  is the set of positive real numbers.  $G_{bx}$  is the mapping function relationship between the transition and its associ-

ated interactive button set  $X$ , namely,  $T_{dt} \rightarrow X$ , which can be defined as  $\forall x \in X, \exists t_{dti} \in T_{dt} | Gbx(t_{dti}) = x$ .

According to the model established above, the graphical description diagram of the model DSAM can be obtained by using the graphical description method. Under the synchronization time constraint of  $T_{t0}$ , the  $P_0$  and  $P_2$  tokens are changed. Under the interactive operation of the Internet of things video data frame  $X_i$ , the changes are further transferred, and the graphical description of the model DSAM shown in Figure 2 is obtained.

**3.2. Model Analysis.** Using  $\pi$ -net theory, the state evolution, transition, and dynamic interaction of the DSAM model are analyzed.

**3.2.1. State Evolution.** When studying the DSAM model, the state of the model should be analyzed first, and the state set of the model should be given; then, the state evolution of the model should be studied on the basis of the state, and the state evolution rules should be given.

**Definition 3.** Model state set definition: the state set of DSAM is represented by  $Ss$ ; then,  $Ss$  is a triple, that is,

$$Ss = (c, T_{det}, K_{ebt}). \quad (3)$$

Among them,  $P_t$  is the location set containing tokens in the model and  $T_{det}$  is the dynamic valid time period table of various information in the model; the number in the table is the same as the number of marked locations; if the user performs a pause operation at a certain moment, the value in  $T_{det}$  is the time remaining at the position;  $K_{ebt}$  is the button list that the user will operate; that is, record the user's optional operations from the present moment to the end.

**Rule 1.** State evolution rule: suppose  $t_{det} \in T_{det}$  is the transition of state  $Ss$  enabled by relative time  $R_t$ ; then, the model can change at the dynamic effective time  $t_{det}$  and evolve into a new state  $Ss'$ , namely,  $Ss' = (P_t', T_{det}', K_{ebt}')$ , as shown in

$$P_t' : (\forall p_k \in P_k) P_t'(p_k) = P_t(p_k) - R_t(t_{det}, p_k) + F_{kz}(t_{det}, p_k). \quad (4)$$

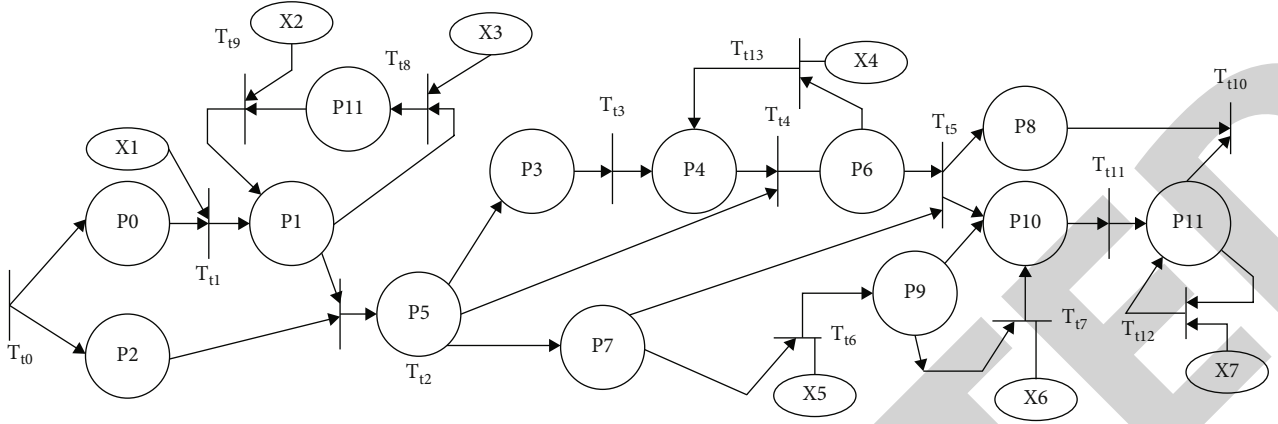


FIGURE 2: Graphical representation of the model DSAM.

$T'_{det}$ :  $T'_{det}$  is the dynamic relative effective time period table of the position marked by  $P'_t$ , and if  $[a_i, n_i, b_i]$  is the time interval of the place  $P_{ki}$  in the state of  $S_s$ , it satisfies the following:

$$\forall p_k \in P_k \wedge P'_t(p_{ki}) > 0, \quad (5)$$

$$T'_{det}(p_{ki}) = \begin{cases} [L_{\max}(0, a_i - \theta), n_i - \theta, L_{\max}(0, b_i - \theta)] P_t(p_{ki}) > 0, \\ [a_i, n_i, b_i] P_t(p_{ki}) = 0, \end{cases} \quad (6)$$

$$K'_{ebt} : \forall t \in T_t, \quad (7)$$

$$K'_{ebt}(t_t) = \begin{cases} x, \exists x \in X \wedge P'_t(p_{kit}) > 0 \wedge X P_t(t_t) = x, \\ \phi. \end{cases} \quad (8)$$

Among them,  $p_{kit}$  is the input position of transition  $T_{dt}$ .

**3.2.2. Model Change.** The transitions of the model DSAM mainly include “Key”-type transitions and non-“Key”-type transitions.

**Definition 4.** Transition occurrence condition: set in time  $\Delta t_t$ , the triggering of transition  $t_{det}$  in  $t_t$  is determined by the state; it must satisfy the following:

- (i)  $t_{det}$  is enabled by  $P_t$  at time point  $\theta_t$ :  $(\forall p_{ki} \in P_k)(P_k(p_{ki}) \geq F_{kz}(p_{ki}, t_{det}))$
- (ii)  $\theta_t$  meets:  $\min(i) \leq \theta_t \leq \min_i(\max(i))$

When the transition conditions given in Definition 4 are met, the transition cannot occur because the time factor is also required. Definition 2 shows that if the time  $T_t$  meets the requirements of the TPN network, the transition  $t_{det}$  can occur.

**Rule 2. Model communication transition rule:** assuming that  $p_{pi}$  and  $p_{pj}$  are a pair of conjugate transitions of the model DSAM, if there are two subnetworks  $Net_1 t$  and  $Net_2$  of the network DSAM that are complementary to each other

and the functions that identify all the place state items of the network DSAM, for any two states belonging to  $S_s$ , there are  $\forall t_1 \in Net_1, t_2 \in Net_2, \exists BS * (t_1) = \alpha_1, BS * (t_2) = \alpha_2$ ; then,  $t_1$  and  $t_2$  can generate communication transition  $t_{tb}$  in the network DSAM, namely,  $t_{tb} = \langle t_1, t_2 \rangle, \omega_t = \xi$  (representing the transition type between various information such as input transition, free output transition, restricted output transition, communication transition, and matching transition), such that  $*t_{tb} = *t_1 \cup *t_2, t_{tb}^* = t_1^* \cup t_2^*, \forall s \in *t_1, C_f(s, t) = C_f(s, t_1)$ , with the rule: let  $\lambda_{r1} = ay\{y/x\}$ , where  $\lambda_{r1}$  is the number of various information of IoT video perception,  $x$  is the label of the output library,  $y$  is the free channel name on the output, and  $a$  is the replacement of the channel name. There are the following:

- (i) When  $\omega_{t2} = ay$ , then  $\omega_t = \xi\{y/x\}$ , and  $\forall s \in t_1^*, C_f(t, s) = C_f(t_1, s)$
- (ii) When  $\omega_{t2} = a(y)$ , then  $\lambda_t = \xi\{y/x\}$ , and  $\forall s \in t_1^*, C_f(t, s) = C_f(t_1, s) + (\varphi, \varphi, \varphi, \{y\})$

**3.2.3. Model Dynamic Interaction.** For the IoT video perception system, the dynamic interaction with users is to realize the synchronization problem of IoT video perception. If the transition accepts the user input button, there is a schematic diagram of the interactive operation as shown in Figure 3 (where  $\{X_1, X_2, X_3, \dots\}$  is the interactive button set  $X$ ).

- (i) “Skip”: if the user input button is “Skip,” the model DSAM transition will be activated immediately, and the library place that is not executing completes the semantics
- (ii) “Pause” and “Restart”: if the user submits a “Pause,” the place  $C_p$  accepts a token and performs a Nop operation at the same time until the next input interaction is “Restart”
- (iii) “Modify Speed”: if the user inputs the “Modify Speed” operation of the library place  $\theta_t$  at time  $C_p$ , the result is to change the execution speed of various information of IoT video perception

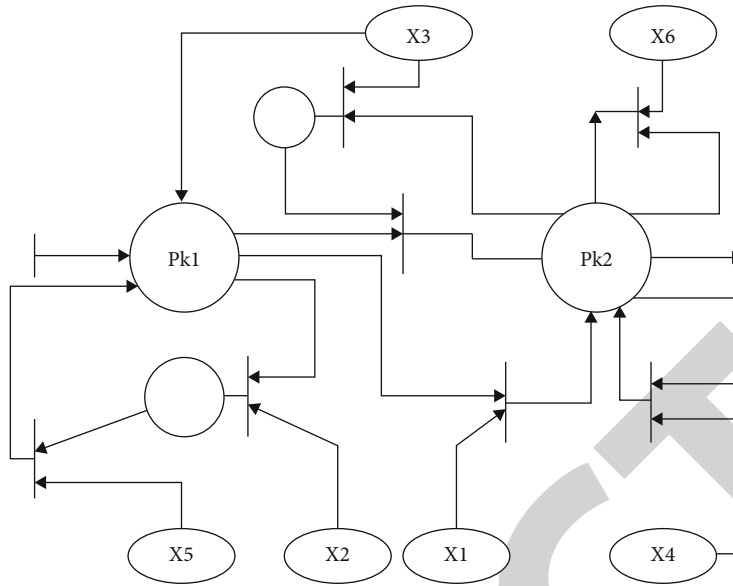


FIGURE 3: Graphical description of the  $\pi$  network for model interaction.

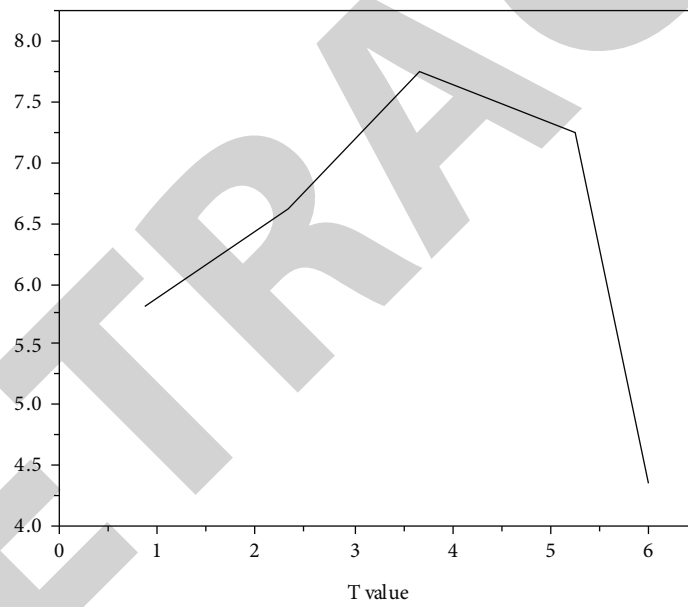
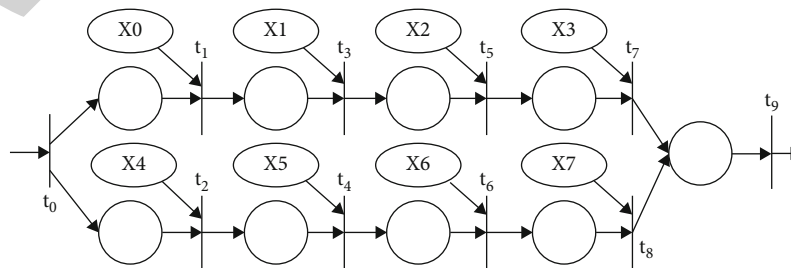
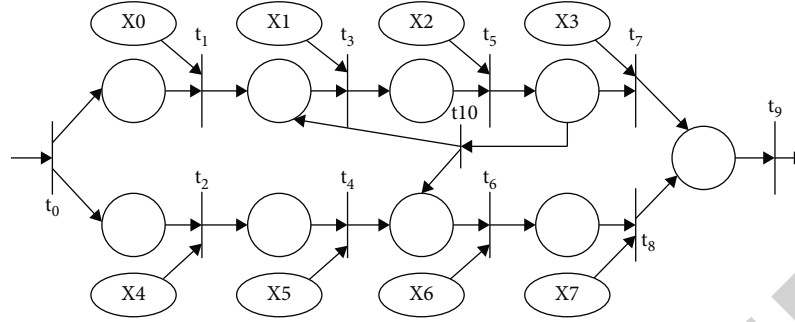


FIGURE 4: Sequence diagram of IoT video perception data flow.



Among them:  $P_i$  represents the  $C_{pi}$  in the model DSAM;  $X_i$  represents the interactive operation;  $t_i$  represents the synchronization time; the arrow represents the transition.

FIGURE 5: DSAM diagram of the audio and video synchronization model.



Among them:  $P_i$  represents the  $C_{pi}$  in the model DSAM;  $X_i$  represents the interactive operation;  $t_i$  represents the synchronization time; the arrow represents the transition.

FIGURE 6: Exception handling of the audio and video synchronization model DSAM.

TABLE 1: Comparison of model DSAM with MTFSC and 3TFSC video intraframe synchronization quantization.

Project	Comparing results								
	50			100			200		
Number of buffer media	DSAM	MTFSC	3TFSC	DSAM	MTFSC	3TFSC	DSAM	MTFSC	3TFSC
$N_{DownFlow}$	15	20	25	8	10	12	2	4	9
$X_{DataLost}$ (%)	1.02	1.50	2.15	1.07	1.98	2.18	1.09	1.99	2.28

TABLE 2: Synchronization comparison between video frames (%).

Project	Comparing results			
	Test time	9:15	9:25	9:35
No synchronization control	Teacher audio and video synchronization	77.23	70.12	71.02
	Teacher audio and screen sync	77.14	75.29	73.25
	On-screen text and teacher audio sync	75.48	69.58	70.46
	Teacher audio and video synchronization	99.12	99.75	99.14
With synchronous control	Teacher audio and screen sync	99.45	99.76	99.46
	On-screen text and teacher audio sync	98.17	99.25	99.74

- (iv) “Back”: the user has entered a back operation, and the result is the IoT video perception information directly back to the previous moment or time period
- (v) “Replay”: if the user input is the “Replay” button, the model DSAM will reexecute various information of the operated IoT video perception

From the above analysis, it can be seen that the DSAM model can well realize and complete the dynamic interaction between media and users [17].

## 4. Analysis of Results

**4.1. Example Simulation.** In order to use the DSAM model to describe the dynamic synchronization problem of IoT video perception, it is assumed that the IoT video perception system is a composite data stream of video, sound, text, and animation; the time series relationship between media objects and subobjects is shown in Figure 4. The user interacts with various information of IoT video perception

through the interaction button set  $X$  [18]. When starting to run, you can directly jump to  $C_{f1}$  for performance, “Pause” and “Restart” Vdo1 performance, return from Vdo3 to Vdo2 for performance, and also make am1 perform again.

The synchronization of audio and video is shown in Figure 5. The audio and video data stream speed is 10 frames per second. The maximum distortion in QoS is 80 ms, and the maximum jitter is 10 ms.

**4.2. Exception Handling.** It can be seen from the example simulation that the maximum distortion and maximum jitter in QoS are caused by the difficulty of fully synchronizing various information of IoT video perception, so it is necessary to use certain methods to process media data streams. The processed sound and video are shown in Figure 6.

In IoT video-aware synchronous communication, data loss due to signal attenuation, interference, and delay is inevitable. In the simulation example, the LDU of the audio stream cannot be discarded arbitrarily for the sound data,

and a suppression arc is introduced for abnormal processing. For video media streams, losing a small amount of data has little effect on video QoS. Therefore, the model is able to implement exception handling and is robust to a certain degree of object loss [19–21].

**4.3. Model Performance Analysis.** To analyze the performance of the model, first analyze the synchronization quantification within the media, and then, analyze the synchronization quantification between the video information. The internal synchronization quantization of the video is analyzed, and its indicators are mainly the buffer underflow times  $N_{\text{DownFlow}}$  and the data information packet loss rate  $X_{\text{DataLost}}$ ; the data shown in Table 1 are obtained through experiments. From the data in Table 1, it can be seen that when the model DSAM is tested and verified, the obtained data buffer underflow times are less than those of the other two models. The packet loss rate of video information data is also lower than that of the other two models. Therefore, the model DSAM has certain advantages in the control of intravideo synchronization.

A quantitative test is carried out on the synchronization between video frames, the test environment uses video images, voice, text, etc., under experimental conditions, and the teacher lectures in the Internet of things video perception classroom are tested, in order to verify video frame synchronization. After experiments, the data shown in Table 2 were obtained. From the data in Table 2, it can be seen that without synchronization control, the synchronization rate between video frames is lower than that with synchronization control [22].

From the above analysis, it can be seen that the model DSAM has excellent performance in both intravideo synchronization control and video interframe synchronization control [23–25].

## 5. Conclusion

Aiming at the dynamic synchronization problem of Internet of things video perception, the authors use the  $\pi$  network combined with the Petri net and  $\pi$  calculus to establish the abstract model DSAM of the Internet of things video perception system and realize the modeling of the dynamic synchronization of the Internet of things video perception system. Through the simulation and analysis of the model DSAM, it can be seen that the model proposed and established by the authors is able to correctly handle the dynamic synchronization of IoT video perception which has certain practical value.

## Data Availability

The data used to support the findings of this study are available from the corresponding author upon request.

## Conflicts of Interest

The authors declare that they have no conflicts of interest.

## References

- [1] Q. Ling, B. Hu, X. Shen, H. Liao, and H. Ni, "Health perception system design based on sensor Internet of things for transmission tower's structure status," *IOP Conference Series: Earth and Environmental Science*, vol. 668, no. 1, article 012080, 2021(7pp).
- [2] T. H. Jo, J. H. Ma, and S. H. Cha, "Elderly perception on the Internet of things-based integrated smart-home system," *Sensors*, vol. 21, no. 4, p. 1284, 2021.
- [3] J. Liu, Y. Duan, Y. Wu, R. Chen, G. Chen, and G. Chen, "Information flow perception modeling and optimization of Internet of things for cloud services," *Future Generation Computer Systems*, vol. 115, no. 8, pp. 671–679, 2021.
- [4] A. H. Sodhro, S. Pirbhulal, Z. Luo, K. Muhammad, and N. Zahid, "Towards 6G architecture for energy efficient communication in IoT-enabled smart automation systems," *IEEE Internet of Things Journal*, vol. 8, pp. 5141–5148, 2020.
- [5] A. Mellit, M. Benganem, O. Herrak, and A. Messaloui, "Design of a novel remote monitoring system for smart greenhouses using the Internet of things and deep convolutional neural networks," *Energies*, vol. 14, no. 16, p. 5045, 2021.
- [6] R. K. Jha, H. Kour, M. Kumar, and S. Jain, "Layer based security in narrow band Internet of things (NB-IoT)," *Computer Networks*, vol. 185, no. 3, article 107592, 2020.
- [7] X. Tang, "Research on smart logistics model based on Internet of things technology," *IEEE Access*, vol. 8, pp. 151150–151159, 2020.
- [8] L. Xing, "Reliability in Internet of things: current status and future perspectives," *IEEE Internet of Things Journal*, vol. 7, no. 8, pp. 6704–6721, 2020.
- [9] H. Zhang, D. Ge, N. Yang, P. Jia, and Y. Yang, "Study on Internet of things architecture of substation online monitoring equipment," in *MATEC Web of Conferences*, vol. 336, Beijing city of China, 2021no. 5, Article ID 05024.
- [10] H. Qin, B. Zhao, L. Xu, and X. Bai, "Hybrid cyber petri net modelling, simulation and analysis of master-slave charging for wireless rechargeable sensor networks," *Sensors*, vol. 21, no. 2, p. 551, 2021.
- [11] X. Pan, Y. Wang, S. He, and K. S. Chin, "A dynamic programming algorithm-based clustering model and its application to interval type-2 fuzzy large-scale group decision making problem," *IEEE Transactions on Fuzzy Systems*, vol. 30, pp. 108–120, 2020.
- [12] A. Sabol, R. Alimo, F. Kamangar, and R. Madani, "Deep space network scheduling via mixed-integer linear programming," *IEEE Access*, vol. 9, pp. 39985–39994, 2021.
- [13] L. Song, Y. Fu, J. Su, K. Zhou, and M. Long, "A novel modeling method of the crowdsourcing design process for complex products-based an object-oriented petri net," *IEEE Access*, vol. 9, pp. 41430–41440, 2021.
- [14] C. W. Chen, "Internet of video things: next-generation iot with visual sensors," *IEEE Internet of Things Journal*, vol. 7, no. 8, pp. 6676–6685, 2020.
- [15] S. Zhao, X. Cheng, and J. Li, "Sensor fault diagnosis based on adaptive arc fuzzy DBN-Petri net," *IEEE Access*, vol. 9, pp. 20305–20317, 2021.
- [16] Y. Hu, X. Qiao, X. Luo, and C. Peng, "Diversified semantic attention model for fine-grained entity typing," *IEEE Access*, vol. 9, pp. 2251–2265, 2020.

- [17] Y. Hara, Y. Jodai, T. Okinaga, and M. Furukawa, "Numerical analysis of the dynamic interaction between two closely spaced vertical-axis wind turbines," *Energies*, vol. 14, no. 8, p. 2286, 2021.
- [18] X. Wang, "Application of 3D-HEVC fast coding by Internet of things data in intelligent decision," *The Journal of Supercomputing*, vol. 78, no. 5, pp. 7489–7508, 2022.
- [19] M. A. Ezzat, M. Ghany, S. Almotairi, and A. M. Salem, "Horizontal review on video surveillance for smart cities: edge devices, applications, datasets, and future trends," *Sensors*, vol. 21, no. 9, p. 3222, 2021.
- [20] J. Zhang, Q. Cui, Z. Zhao, and S. Huo, "Synchronization control design based on observers for time-delay Lur'e systems," *IEEE Access*, vol. 8, pp. 92886–92894, 2020.
- [21] M. Fan and A. Sharma, "Design and implementation of construction cost prediction model based on SVM and LSSVM in industries 4.0," *International Journal of Intelligent Computing and Cybernetics*, vol. 14, no. 2, pp. 145–157, 2021.
- [22] S. Shriram, J. Jaya, S. Shankar, and P. Ajay, "Deep learning-based real-time AI virtual mouse system using computer vision to avoid COVID-19 spread," *Journal of healthcare engineering*, vol. 2021, 8 pages, 2021.
- [23] L. Xin, L. Jianqi, C. Jiayao, Z. Fangchuan, and C. Ma, "Study on treatment of printing and dyeing waste gas in the atmosphere with CeMn/GF catalyst," *Arabian Journal of sciences*, vol. 14, no. 8, pp. 1–6, 2021.
- [24] R. Huang, P. Yan, and X. Yang, "Knowledge map visualization of technology hotspots and development trends in China's textile manufacturing industry," *IET Collaborative Intelligent Manufacturing*, vol. 3, no. 3, pp. 243–251, 2021.
- [25] Z. Guo and Z. Xiao, "Research on online calibration of lidar and camera for intelligent connected vehicles based on depth-edge matching," *Nonlinear Engineering*, vol. 10, no. 1, pp. 469–476, 2021.